Magnetic ordering of the Mn sublattice: Dense Kondo-lattice behavior of Ce in $(R\mathrm{Pd}_3)_8\mathrm{Mn}$ (R=La,Ce)

Surjeet Singh* and S. K. Dhar†
CMP&MS, TIFR, Homi Bhabha Road, Mumbai 400 005, India
(Received 30 March 2003; revised manuscript received 7 July 2003; published 27 October 2003)

We have synthesized interstitial compounds $(R\mathrm{Pd}_3)_8\mathrm{Mn}$ (R=La and Ce). The Mn ions in these compounds, present in ''dilute'' concentrations of just 3 molar percent, form a regular sublattice with an unusually large Mn-Mn near-neighbor distance of ~8.5 Å. While the existence of $(R\mathrm{Pd}_3)_8M$ (M: p-block element) is already documented in the literature, the present work reports on the formation of this phase with M being a $3d$ element. In $(\mathrm{LaPd}_3)_8\mathrm{Mn}$, the Mn sublattice orders antiferromagnetically, as inferred from the peaks in low-field magnetization at 48 and 23 K. The latter peak progressively shifts towards lower temperatures in increasing magnetic field and disappears below 1.8 K in a field of ~8 kOe. On the other hand, in $(\mathrm{CePd}_3)_8\mathrm{Mn}$ the Mn sublattice undergoes a ferromagnetic transition around 35 K. The Ce ions form a dense Kondo lattice and are in a paramagnetic state at least down to 1.5 K. A strongly correlated electronic ground state, arising from the Kondo effect, is inferred from the large extrapolated value of $C/T=275$ mJ/mol Ce K^2 at $T=0$ K.

DOI: 10.1103/PhysRevB.68.144433 PACS number(s): 75.20.Hr, 71.27.+a, 75.30.Cr, 75.47.Np

I. INTRODUCTION

$R\mathrm{Pd}_3$ compounds have AuCu_3-type crystal structure with R and Pd atoms occupying the corners ($1a$) and face centers ($3c$) of the cubic unit cell, respectively. A unique way of alloying $R\mathrm{Pd}_3$ (R=La to Lu) compounds was reported by Dhar *et al.*, when they observed that smaller p-block atoms such as boron could be incorporated interstitially in the $R\mathrm{Pd}_3$ crystal lattice.[1] The smaller boron atoms occupy the interstitial body-center position (for the sake of brevity we will refer to it as the $1b$ site) in the RPd_3 unit cell forming a defect pervoskite-type structure with formula $R\mathrm{Pd}_3\mathrm{B}_x$ ($0<x<1$). It was later found that silicon could also be incorporated in the $R\mathrm{Pd}_3$ unit cell up to $x\sim0.3$.[2] Alloying with boron and silicon resulted in the expansion of the lattice and drastically changed the valence and hence the magnetic properties of CePd_3 and EuPd_3.[1–5] Briefly, cerium ions changed from a valence fluctuating state in CePd_3 to a trivalent state in $\mathrm{CePd}_3\mathrm{B}_x$ for $x>0.12$, while the lattice expansion forced the europium ions to change from the trivalent state in EuPd_3 to the valence fluctuating state in $\mathrm{EuPd}_3\mathrm{B}_x$ alloys, with possible charge ordering in $\mathrm{EuPd}_3\mathrm{B}$.

An interesting extension of the abovementioned interstitial alloying has recently been reported by Gordon and DiSalvo.[6] They found that alloying CePd_3 with an appropriate amount of Sb leads to the formation of a cubic superstructure $(\mathrm{CePd}_3)_8\mathrm{Sb}$ closely related to the AuCu_3-type structure of CePd_3. The large sized Sb atoms deform the Pd octahedra, such that the available $1b$ sites in the CePd_3 lattice are occupied by Sb atoms only in a regular pattern forming a simple-cubic sublattice with near neighbor Sb-Sb separation slightly more than twice the lattice parameter of the parent CePd_3 unit cell. In the superstructure the Ce atom remains coordinated by 12 Pd atoms and the Ce-Ce separation is increased by 2 to 3% over its value in CePd_3. A rigorous discussion of the superstructure is given in Refs. 6, 7. Later, it was found that the superstructure $(\mathrm{CePd}_3)_8M$ is also formed for other p-block elements M=Ga, In, Sn, Pb, and Bi, and for $(\mathrm{LaPd}_3)_8\mathrm{In}$.[8] $(\mathrm{CePd}_3)_8M$ compounds order magnetically below 10 K in contrast to the Pauli paramagnetic, valence fluctuating ground state in CePd_3, and they exhibit heavy-fermion-like enhanced low temperature electronic specific heat coefficient γ.[9–11] Further investigations showed that $(\mathrm{CePd}_3)_8M$ (M=Al and Ge) also form, order magnetically below 10 K, and exhibit a dense Kondo lattice behavior.[7,10,12] Jones *et al.* also attempted synthesis of $(\mathrm{CePd}_3)_8M$ for M=Zn and Te.[10] Though their powder x-ray diffraction patterns showed the signature of superstructure formation, there were some doubts about the homogeneity and the exact stoichiometry of the samples. The case for M=Zn is interesting in the sense that Zn is not a p-block element which motivated us to search for other atoms in the $3d$ series that might lead to superstructure formation.

In the present work, we report on the formation of ''dilute-Mn'' ternary compounds $(R\mathrm{Pd}_3)_8\mathrm{Mn}$ for R=La and Ce. The word ''dilute'' emphasizes the fact that the Mn concentration in these compounds is low (about a few molar percent) and yet the Mn ions form a periodic lattice with unusually large nearest neighbor Mn-Mn separation allowing localization of the $3d$ moments. Recently such ''dilute-Mn'' compounds have attracted considerable attention. Negative colossal magnetoresistance has been reported in the single crystals of Zintl compounds $\mathrm{Eu}_{14}\mathrm{MnSb}_{11}$ and $\mathrm{Eu}_{14}\mathrm{MnBi}_{11}$, despite antiferromagnetic ordering in the latter compound.[13] In $\mathrm{Yb}_{14}\mathrm{MnSb}_{11}$ (where Yb ions are divalent and hence nonmagnetic) the localized Mn^{3+} moments are coupled via conduction electrons and order ferromagnetically at 53 K.[14,15] $\mathrm{Yb}_{14}\mathrm{MnBi}_{11}$ exhibits two magnetic transitions: a ferromagnetic transition at 58 K followed by a second transition at 28 K.[14] It was pointed out in Ref. 14 that similar ''dilute'' intermetallic compounds may be a good starting point to find $3d$-Kondo-lattice systems, analogous to the well known and extensively studied $4f$ Kondo-lattice/heavy fermion systems. We find that in $(R\mathrm{Pd}_3)_8\mathrm{Mn}$ (R=La,Ce) the nearest neighbor Mn-Mn separation is unusually large ~8.5 Å. In $(\mathrm{LaPd}_3)_8\mathrm{Mn}$ the Mn ions are in a localized 2+ valence state

and order antiferromagnetically below ~50 K. In $(CePd_3)_8Mn$ the Ce ions form a dense Kondo lattice and do not order magnetically at least down to 1.5 K. However, the Mn sublattice orders ferromagnetically near 35 K.

II. EXPERIMENT

The composition $(RPd_3)_8Mn$ for $R=$La and Ce were synthesised by the standard technique of arc melting in an inert atmosphere of argon. First an ingot of RPd_3 was melted and then Mn added to it by gently focusing the arc on the pellet of RPd_3 so that Mn, which is volatile, was not directly heated. The button of the ternary alloy was flipped over and remelted several times to ensure homogenization. The initial and final weights of the pellets are practically the same and hence there is no loss of Mn. We believe that the success of the arc melting technique for making these samples is partially due to the fact that the molar percentage fraction of Mn is low (~3%). The samples were checked for their phase purity by the standard powder x-ray diffraction technique and optical micrography. The resistance between 1.5–300 K was measured by the four-probe dc method on a rectangular parallelepiped piece of the uniform cross section. Contacts with the sample were made using gold wire and silver paste. The following method was used to remove the uncertainty in the value of resistivity arising due to the error associated with the measurement of distance between the voltage probes. The two current and one voltage probes were fixed to the sample, the room-temperature resistance (R) of the sample was then measured as a function of distance by moving the second voltage probe in fixed steps of $\delta L = 0.05$ mm. The slope of the R vs $L+\delta L$ (where L is the initial distance between the moving and fixed voltage probes; the slope is independent of the choice of L) is used to normalize the value of resistivity obtained from silver contact measurements. The heat capacity was measured by using the semiadiabatic, heat pulse method. Magnetization as a function of temperature and field was recorded by using VSM (Oxford Instruments) and SQUID (Quantum Design) magnetometers.

III. RESULTS AND DISCUSSIONS

A. Powder x-ray diffraction patterns

A representative powder x-ray diffraction pattern of $(LaPd_3)_8Mn$ obtained using Cu-$K\alpha$ radiations is shown in Fig. 1. The crystal structure was refined using the Rietveld refinement program FULLPROF (Ref. 16) and an output of such a fitting is also presented in Fig. 1. The Bragg peaks for the powder pattern of $(LaPd_3)_8Mn$, generated by the FULLPROF, are shown as two sets of vertical bars in Fig. 1. While the bigger and thicker bars correspond to the reflections one would expect from a face centered cubic $LaPd_3$ lattice, the smaller bars (labeled as satellite peaks in the figure) correspond to additional low intensity satellite peaks arising due to the periodic occupation of $1b$ sites by the bigger Mn atoms resulting in the formation of a cubic superstructure of size about twice the size of the $LaPd_3$ unit cell. The powder diffraction pattern of $(CePd_3)_8Mn$, similarly, showed the formation of cubic superstructure. The lattice parameters a of $(LaPd_3)_8Mn$ and $(CePd_3)_8Mn$ are 8.466 and 8.415 Å respectively, which is also the nearest neighbor Mn-Mn separation in the two compounds. We find that the superstructure in $(RPd_3)_8Mn$ ($R=$La and Ce) is sensitive to the heat treatment. For example, annealing the $(CePd_3)_8Mn$ samples at 900°C diminishes the low intensity satellite peaks and gives rise to new peaks, indicating a degradation of the phase by the heat treatment. All the data reported in this work were taken on the as-cast samples.

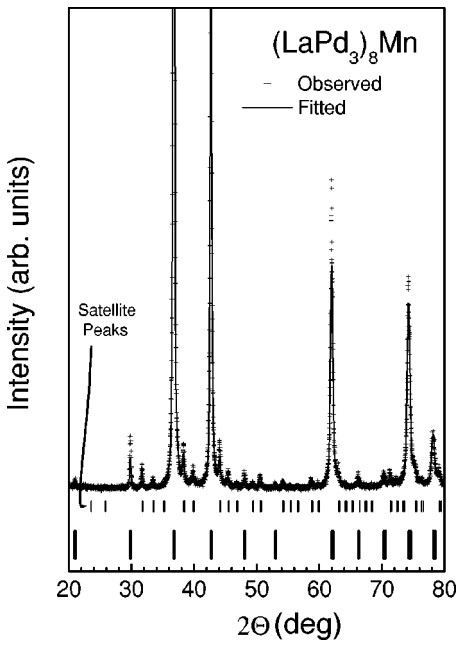

FIG. 1. The observed (cross) and fitted (solid line) powder x-ray diffraction pattern of $(LaPd_3)_8Mn$. The vertical bars indicate the position of the Bragg peaks.

B. $(LaPd_3)_8Mn$

$LaPd_3$ is diamagnetic at room temperature and shows a nearly temperature independent magnetic susceptibility.[17] The inverse molar susceptibility χ^{-1} of $(LaPd_3)_8Mn$ measured in an applied field of 3 kOe is shown in Fig. 2. Between 100 and 300 K the data can be fitted to a modified Curie-Weiss expression $\chi=\chi_0+C/(T-\Theta_p)$, where C is the Curie constant and χ_0 is the temperature-independent contribution to the total magnetic susceptibility and Θ_p is the paramagnetic Curie temperature. The values of the best-fit parameters are $\mu_{\text{eff}}=5.9\mu_B$/f.u. (derived from C), $\Theta_p = 52.1$ K, and $\chi_0=-0.003$ emu/mol. The μ_{eff} is comparable to the theoretical value of 5.92 μ_B for Mn^{2+} ($S=5/2$) ion and suggest that the Mn ions in this compound are in a $3d^5$ electronic configuration. The negative χ_0 (about 20% of the total susceptibility at 300 K) arises from the diamagnetic contribution of the $LaPd_3$ network and is comparable to the susceptibility of $(LaPd_3)_8In$ which is reported to be -1.06×10^{-3} emu/mol at 293 K.[8] The susceptibility of $(LaPd_3)_8Mn$ measured in a field of 1 kOe is shown in the inset of Fig. 2. At low temperatures the susceptibility shows a peak at 48 K ($T1$) indicating an antiferromagnetic transi-

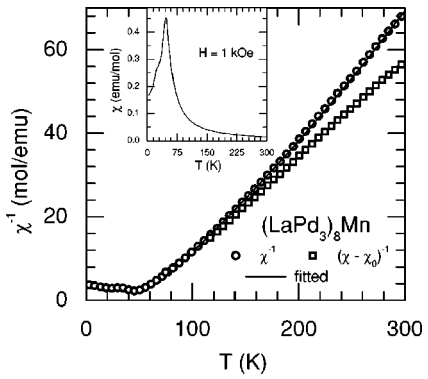

FIG. 2. The inverse molar susceptibilities χ^{-1} and $(\chi-\chi_0)^{-1}$ of $(LaPd_3)_8Mn$ as a function of temperature. χ_0 is estimated by fitting the susceptibility data to the modified Curie-Weiss expression (refer to the text for details). The line is the best-fit of the data to the modified Curie-Weiss expression. Inset: The temperature variation of the magnetic susceptibility of $(LaPd_3)_8Mn$ measured in an applied field of 1 kOe between 1.5 and 300 K.

tion. In addition there is a smaller peak at 23 K ($T2$) indicative of a second phase transition.

Figure 3(a) shows that the magnetization of $(LaPd_3)_8Mn$ measured in zero-field-cooled (ZFC) and field-cooled (FC) modes in an applied field of 100 Oe is practically the same. Further, we do not observe any frequency dependence of the ac susceptibility measured at 1, 9, and 99 Hz [Fig. 3(b)]. These data show conclusively that the peaks in the magnetization arise due to the long-range magnetic order and not due to any spin-glass-type freezing of the Mn moments. The

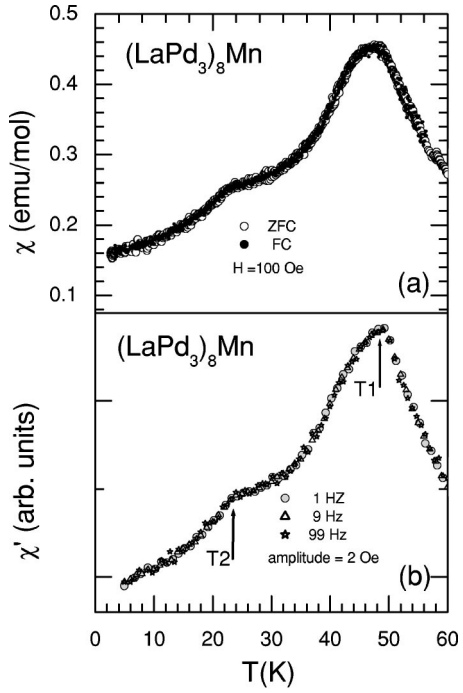

FIG. 3. The magnetic susceptibility of $(LaPd_3)_8Mn$ as a function of temperature: (a) dc susceptibility (χ) in zero-field-cooled (ZFC) and field-cooled (FC) modes in an applied field of 100 Oe. (b) ac susceptibility (χ') at 1, 9, and 99 Hz.

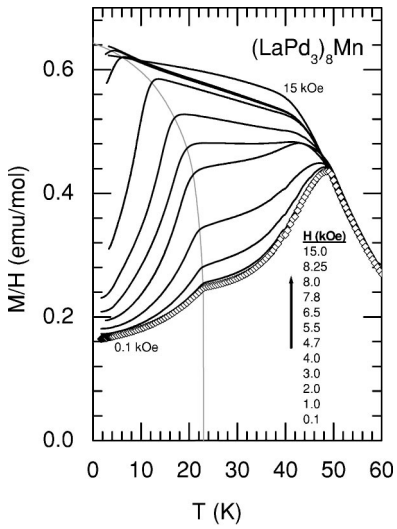

FIG. 4. The magnetization (M/H) of $(LaPd_3)_8Mn$ as a function of temperature for a number of fixed applied fields. The dotted line (guide to the eye) trace the locus of the $T2$ peak which shift towards lower temperatures with increase in the applied magnetic field.

magnetization $[M(T)/H]_H$ of $(LaPd_3)_8Mn$, measured in several applied fields below 60 K is depicted in Fig. 4. $[M(T)/H]_H$ in the ordered state exhibits very unusual behavior in relatively low applied fields. Noteworthy is the shift of the $T2$ peak to lower temperatures: above $\sim$3 kOe the $T2$ peak shifts rapidly to lower temperatures and disappears below 1.8 K in an applied field of $\sim$8.25 kOe. The magnitude of M/H, on the other hand, increases with the increase in the magnetic field.

The isothermal magnetization $[M(H)]_T$ measured at several temperatures between 2 and 50 K is shown in Fig. 5. For each T, $[M(H)]_T$ is measured by cooling the sample from above 60 K to the desired temperature in a nominal zero

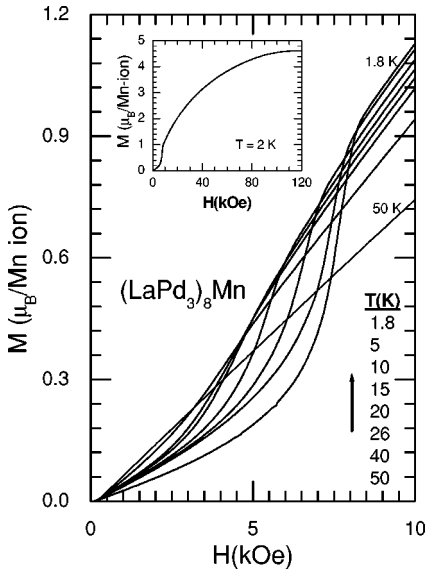

FIG. 5. The magnetization isotherms of $(LaPd_3)_8Mn$ as a function of applied magnetic field at several temperatures. Inset: data plotted up to 120 kOe at 2K.

field. $[M(H)]_{1.8\,\mathrm{K}}$ undergoes a sharp metamagnetic transition in a ''critical field'' of ~ 8.25 kOe, at which the $T2$ peak of magnetization disappears as seen in Fig. 4. At higher temperatures the metamagnetic transition becomes less sharp and the corresponding field at which the metamagnetic transition occurs also decreases. The linearity of the magnetization at 50 K characterizes the response in the paramagnetic state. $[M(H)]_{2\mathrm{K}}$ (shown as inset in Fig. 5 up to 120 kOe) has a tendency towards saturation attaining a value of $\mu_s = 4.6\ \mu_B/\mathrm{Mn}$ in 120 kOe (close to the theoretical value of $5\mu_B$ for Mn^{2+} ion). From the values obtained for μ_{eff} and μ_s we conclude that the $3d$ state of the Mn ions in $(LaPd_3)_8Mn$ has a localized character in contrast to the usual bandlike character of the Mn $3d$ state in the intermetallics.

It may be noticed that though Θ_p obtained from the high temperature Curie-Weiss behavior of the susceptibility data is positive, indicative of ferromagnetic correlations, the peak in χ at $T1$ and the nature of isothermal magnetization suggest antiferromagnetic ordering. The data presented in Figs. 4 and 5 shows that the antiferromagnetic state is not robust. We speculate that the ferromagnetic and antiferromagnetic interactions are competing in this compound. It is worthy of mention here that the Mn sublattice in $(CePd_3)_8Mn$ orders ferromagnetically (see below) and our preliminary investigations reveal a ferromagnetic ground state in $(LaPd_{2.75}Rh_{0.25})_8Mn$ and $(LaPd_{2.75}Ag_{0.25})_8Mn$. Thus it appears that the nature of magnetic ordering is rather sensitively dependent on slight variations in lattice parameter, conduction electron concentration, etc.

It is interesting to note here that the metamagnetic transitions observed in $(LaPd_3)_8Mn$ is qualitatively similar to that observed in bilayer itinerant metamagnet $Sr_3Ru_2O_7$ where the quantum critical fluctuations associated with the metamagnetism at very low temperatures has been shown to give rise to a non-Fermi-liquid behavior in magnetotransport.[18,19] Therefore, it will be very interesting and pertinent to investigate transport and magnetic properties of $(LaPd_3)_8Mn$ at very low temperatures and in fields close to the ''critical field'' ~ 8.25 kOe: the field at which the $T2$ peak in magnetization disappears below 1.8 K or the isothermal magnetization exhibits metamagnetic transition at 1.8 K. We present here our preliminary results on the magnetotransport measurements of $(LaPd_3)_8Mn$ down to 1.5 K.

The zero-field resistivity $\rho(H=0,T)$ data of $(LaPd_3)_8Mn$ between 1.5–300 K are shown in the inset of Fig. 6. A rather low residual resistivity of $\sim 7\ \mu\Omega$cm and a moderately good residual resistivity ratio of about 4.5 is observed. At high temperatures $\rho(0,T)$ decreases almost linearly with temperature down to 100 K. The magnetic transition at $T1$ is clearly reflected by a distinct change in the slope around 48 K below which $\rho(0,T)$ drops precipitously due to the loss of spin-disorder scattering. Around $T2 = 23$ K the zero-field resistivity is smooth with no discernible anomaly. The magnetoresistivty (MR) measured at few selected fields (Fig. 6) shows interesting features, which correlate nicely with the changes in magnetization in applied fields. The MR, measured in applied fields of 7 and 10 kOe, is positive between the temperatures corresponding to $T1$ and $T2$ peaks in the low field

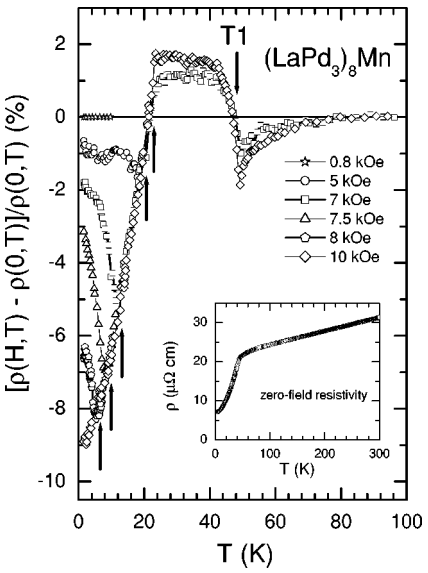

FIG. 6. The magnetoresistance (MR) of $(LaPd_3)_8Mn$ is shown as a function of temperature for several fixed applied fields. The arrows (pointing upward) mark the position of $T2$ peak which shift towards lower temperatures with increasing applied fields. Inset: zero-field resistivity as a function of temperature up to 300 K.

magnetization, in accordance with the positive MR typically observed in the antiferromagnetic state. However, at lower temperatures the MR changes sign and exhibits a field dependent peak, the peak position $T2$ coinciding with that in the dc magnetization at the same value of the applied field. The low temperature peak in MR vanishes for fields above ~ 8.25 kOe within the temperature range of our measurements, thus mimicking the corresponding behavior seen in the dc magnetization. Thus, while the zero-field resistivity is apparently featureless at $T2 = 23$ K, the in-field resistivity changes distinctly at (field dependent) $T2$ pointing at the bulk nature of changes taking place at $T2$.

The in-field resistivity measured at selected fields are plotted in Fig. 7(a) as a function of T^2. The zero-field resistivity and the resistivity in applied fields greater than the ''critical field'' (namely, 8.5, 10, and 15 kOe) follows a T^2 variation between 1.5 and 10 K (T^2 behavior in zero-field persists up to nearly 15 K). The data in 10 and 15 kOe are nearly coincident with the 8.5 kOe data and are, therefore, not shown in the figure. Evidently, for applied fields less than the ''critical field'' (namely, 5, 7.8, and 8 kOe) a similar quadratic dependence of resistivity is not observed at low temperatures. However, at temperatures above the field dependent $T2$ peak the data nearly coincides with the data taken in 8.5 kOe and thus follow a T^2 behavior. MR at a fixed temperature of 1.6 K was measured up to 60 kOe and is shown in Fig. 7(b). MR drops precipitously to -10% at ~ 8.25 kOe, correlating with the metamagnetic transition (Fig. 5). In $Sr_2Ru_3O_7$ also the metamagnetism is similarly observed in the MR.[18] In higher fields the MR becomes less negative attaining a value of -3% at 60 kOe. It would be interesting to study the thermal variation of the magnetoresistivity in magnetic field near the ''critical field'' at very low temperatures for possible non-Fermi-liquid behavior.

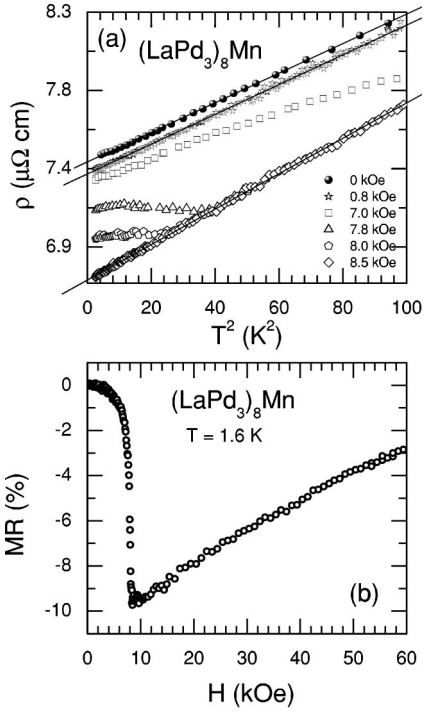

FIG. 7. (a) The in-field resistivity (ρ) of $(LaPd_3)_8Mn$ as a function of T^2 for several fixed applied fields. Lines indicate a quadratic behavior of ρ in T. (b) The magnetoresistance (MR) of $(LaPd_3)_8Mn$ as a function of applied magnetic field at 1.6 K.

The heat capacity C of $(LaPd_3)_8Mn$, shown in Fig. 8 increases monotonically with temperature up to 60 K. No discernible anomaly is seen at $T1$ and $T2$, where the Mn sublattice undergoes transitions. Recalling that the heat capacity at a bulk magnetic transition for spin $S=1/2$ shows a peak of 25 J/mol K in the mean-field approximation, the lack of anomaly at first appears puzzling. However, it should be noticed that in $(LaPd_3)_8Mn$ the Mn ions are just about 3 molar percent. Therefore, the total heat capacity at high temperatures is predominantly due to the phonons. The background lattice heat capacity masks the anomaly expected at the magnetic transitions near $T1$ and $T2$. The heat capacity of isostructural nonmagnetic analog $(LaPd_3)_8Ga$ is also shown in Fig. 8. Assuming that the conduction electron density of states and the phonon contributions in $(LaPd_3)_8Mn$ are exactly the same as in isostructural $(LaPd_3)_8Ga$, we have extracted the excess magnetic contribution C_{mag}, by subtracting the two heat capacities, which is shown in the upper inset of Fig. 8. The relatively poor quality of C_{mag} is easy to understand. Typically, our heat capacity setup has accuracy to within 3–4 %. Subtracting the heat capacities of the two compounds will give large statistical errors ($\sim$10–20 J/mol K) at high temperatures ($C=250$ J/mol K at $\sim$50 K). A peak in C_{mag} centered at 48 K ($=T1$) is indeed seen though no apparent anomaly is observed at $T2$ as in the zero-field resistivity. In the low temperature region ($3<T<6$ K), C/T vs T^2 of $(LaPd_3)_8Mn$ shows linear behavior (see lower inset of Fig. 8) with least square fitted values of $\gamma=57.8\pm1.6$ mJ/mol K^2 and $\beta=6.75\pm0.1$ mJ/mol K^4, where γ and β have their usual meaning. For antiferromagnets the

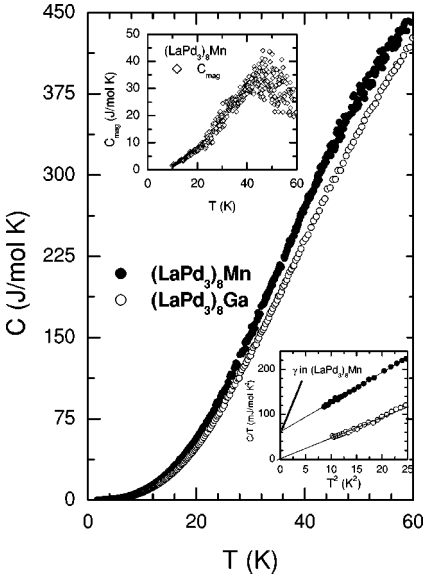

FIG. 8. The heat capacity (C) of $(LaPd_3)_8Mn$ and its nonmagnetic analog $(LaPd_3)_8Ga$ shown as a function of temperature. Upper inset: magnetic part (C_{mag}) of the heat capacity in $(LaPd_3)_8Mn$. Lower inset: C/T plotted against T^2 for the two compounds. The lines are linear extrapolation of the data to $T=0$ K.

spin wave contribution varies as T^3 and should therefore not affect the value of γ. For the nonmagnetic analog $(LaPd_3)_8Ga$ $\gamma=2.3\pm2.1$ mJ/mol K^2 which is comparable to 2.21 mJ/mol K^2 in $(LaPd_3)_8In$ reported by Cho *et al.*[9] The data between 3 and 10 K were least square fitted by including additional T^4 and T^6 terms in the expression for C/T. The values of γ thus obtained are 61.2 ± 5.3 and 5.4 ± 3.3 mJ/mol K^2 for Mn and Ga compounds, respectively. Within the limits of error the two sets of values are comparable for each compound. The value of γ for $(LaPd_3)_8Mn$ is an order of magnitude larger than the corresponding value for $(LaPd_3)_8Ga$ and shows that there is an enhancement in the electronic density of states at the Fermi level in the Mn compound.

The aforementioned features witnessed in the magnetic behavior of $(LaPd_3)_8Mn \equiv LaPd_3Mn_{0.125}$ appear even more striking if one looks at Fig. 9, where the ac susceptibility data of $LaPd_3Mn_{0.06}$ taken at 1, 9, 99, and 999 Hz is

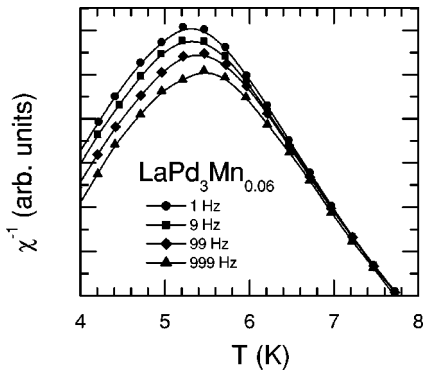

FIG. 9. The ac susceptibility (χ') of $LaPd_3Mn_{0.06}$ measured at 1, 9, 99, and 999 Hz as a function of temperature.

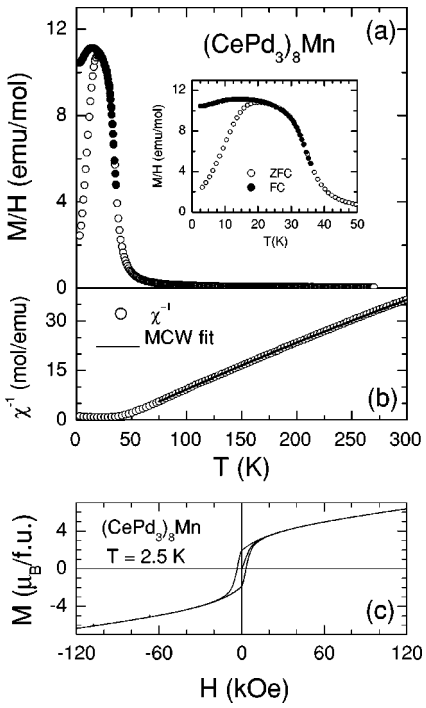

FIG. 10. (a) The magnetization (M/H) of $(CePd_3)_8Mn$ in an applied field of 1 kOe as a function of temperature in zero-field-cooled (ZFC) and field-cooled (FC) mode. Inset: an exaggerated view of the low temperature maximum in M/H. (b) The inverse molar susceptibility in an applied field of 5 kOe as a function of temperature. The solid line is best-fit of the data to the modified Curie-Weiss expression (c) The hysteresis loop in the isothermal magnetization (M) of $(CePd_3)_8Mn$ measured at 2.8 K as a function of applied magnetic field.

shown.[20] In contrast to the long-range magnetic ordering in $LaPd_3Mn_{0.125}$, the alloy $LaPd_3Mn_{0.06}$, where Mn ions are distributed statistically over the available $1b$ sites, exhibits a *spin glass* freezing at 5.5 K as inferred from the frequency dependent peak shift in the ac-χ data.[20]

C. $(CePd_3)_8Mn$

$CePd_3$ is an archetypal valence fluctuating compound with enhanced Pauli-paramagnetic ground state ($\chi \sim 10^{-3}$ emu/mol and $\gamma = 50$ mJ/mol K^2 as $T \to 0$ K).[21–24] Figure 10(a) shows the ZFC and the FC magnetization of $(CePd_3)_8Mn$ in an applied field of 1 kOe. The magnetization increases sharply below 50 K like in a ferromagnetic transition and exhibits a broad peak at 20 K in the ZFC mode. There is a pronounced difference between the ZFC and FC magnetization below the peak temperature. The field dependence of magnetization at 2.8 K, shown in the inset of Fig. 10(c), is characterized by both hysteresis and a high coercive field of 6 kOe. Néel has shown that the magnetization $M(T)$ of a ferromagnet below its Curie temperature T_c in applied field h much smaller than the coercive field $h_c(T)$ is approximately given by the relation $M(T) \approx m_s(T)h^2/h_c^2(T)$, where $m_s(T)$ is the saturation magnetization.[25] Therefore, if below T_c the anisotropy or the coercive field builds up at a rate much faster than $m_s(T)$ then $M(T)$ should show a peak at some temperature. We believe the broad peak at 20 K in ZFC data arises due to the appreciable coercivity/anisotropy in this ferromagnetic material. The FC data in such cases typically show a ferromagnetic saturation below the peak but we find that in $(CePd_3)_8Mn$ the FC magnetization decreases by about 5% below 12 K; the reasons for this are not clear to us. The susceptibility of $(CePd_3)_8Mn$ measured in an applied field of 5 kOe is shown in Fig. 10(b). The data above 75 K can be satisfactorily fitted to the modified Curie-Weiss law. The best-fit parameters obtained from such a fitting are $\chi_0 = 0.002$ emu/f.u., $\mu_{\rm eff}^{\rm observed} = 7.15\mu_B$/f.u. and $\theta_p = +38.7$ K. The positive value of θ_p indicates ferromagnetic interactions. Indeed the Mn sublattice in $(CePd_3)_8Mn$ orders ferromagnetically around 32 K (refer to the Arott plot analysis and heat capacity section below). To deduce the effective magnetic moment per Ce ion it is reasonable to assume that the valence of Mn in $(CePd_3)_8Mn$ is the same as observed in the isomorphous $(LaPd_3)_8Mn$. We further assume that in the paramagnetic regime the contribution of Ce and Mn to the observed effective magnetic moment is simply additive and, therefore, it can be expressed as $\mu_{\rm eff}^{\rm observed} = \sqrt{8(\mu_{\rm eff}^{\rm Ce})^2 + (\mu_{\rm eff}^{\rm Mn})^2}$, where $\mu_{\rm eff}^{\rm Ce}$ and $\mu_{\rm eff}^{\rm Mn}$ are effective magnetic moments per Ce and Mn ions, respectively, in $(CePd_3)_8Mn$. Since in $(LaPd_3)_8Mn$ the effective magnetic moment per Mn ion is $5.9\mu_B$, using this relation we get $\mu_{\rm eff}^{\rm Ce} = 2.42\mu_B$ per Ce ion, which is close to the theoretical value of $2.54\mu_B$ for a free Ce^{3+} ion. Indicating that the valence of Ce in $(CePd_3)_8Mn$ is close to $+3$.

Figure 11(a) shows $[M(H)]_T$ at various temperatures. In Fig. 11(b) we have replotted the data as H/M vs M^2 at $T = 20$, 30, 40, and 45 K. Such plots, known as Arrott plots, are useful in determining the Curie temperature of a ferromagnet. For a ferromagnet the Arrott plot at T_c should pass through the origin while the plots for $T < T_C$ will cut the horizontal axis at a nonzero value, which is the square of the spontaneous magnetization of the ferromagnet (M_s). The plots for $T > T_C$ do not intercept the horizontal axis, since the spontaneous magnetization is zero. Following the standard procedure (see, for example, Ref. 26), the high-field (higher than 5 kOe) data for each temperature is fitted to a fourth order polynomial in M^2 which is extrapolated to determine M_s^2. We find M_s at 40 K is zero while it has a nonzero value at 30 K, indicating that the ferromagnetic ordering temperature of $(CePd_3)_8Mn$ lies between these two temperatures. Isothermal magnetization data at few more temperatures between 30 and 40 K are required to locate T_C exactly. The magnetization at 2.8 K does not saturate even in 120 kOe and its field variation suggests a component varying almost linearly with the field. We believe that the linear component arises from the contribution due to the Ce ions which are in the paramagnetic state down to, at least, 1.5 K (see below, heat capacity and resistivity data). We thus attribute the ferromagnetic transition in $(CePd_3)_8Mn$ to the Mn sublattice. The magnetization at 2.8 K in 120 kOe is $6.4\mu_B$/f.u. and exceeds the corresponding value in $(LaPd_3)_8Mn$ substantially due to the (paramagnetic) contribution from the Ce sublattice.

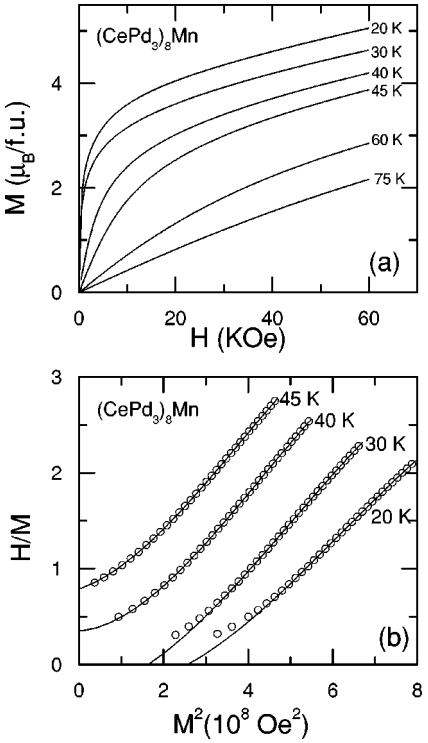

FIG. 11. The magnetization isotherms of $(CePd_3)_8Mn$ at several temperatures between 20 and 75 K are shown as a function of temperature. (b) Arrot plots at 20, 30, 40, and 45 K in $(CePd_3)_8Mn$. The continuous lines are polynomial (in M^2) fits to the high field data (please see text for details).

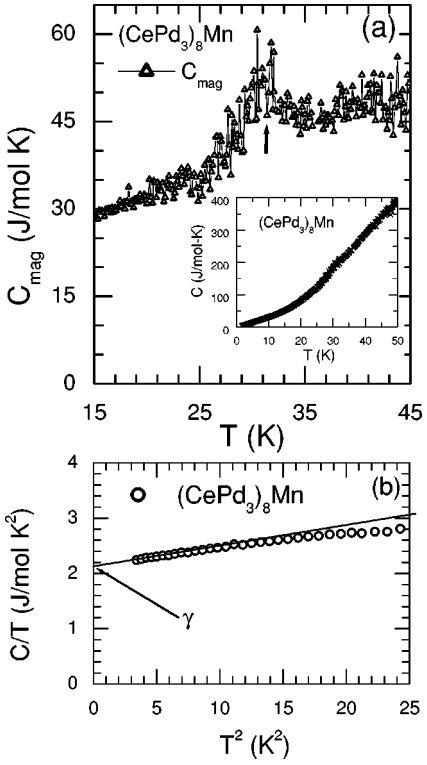

FIG. 13. (a) The magnetic part (C_{mag}) in the heat capacity of $(CePd_3)_8Mn$ is shown as a function of temperature between 15 and 45 K. Inset: heat capacity (C) of $(CePd_3)_8Mn$ is shown between 1.5 and 50 K. (b) C/T against T^2 at low temperatures. The line is linear extrapolation of the data to $T=0$ K.

The resistivity (ρ) of $(CePd_3)_8Mn$ (Fig. 12) is about four times larger than that of $(LaPd_3)_8Mn$ at 300 K and its thermal variation is qualitatively similar to that seen in the dense Kondo lattice compounds. The relatively higher ρ in $(CePd_3)_8Mn$ arises from the incoherent Kondo spin disorder scattering. The peak at 16 K is not due to any phase transition as both the heat capacity (see below) and magnetization data do not show any anomaly at that temperature, but it is due to the transition from the incoherent to coherent Kondo scattering regime as seen, for example, in archetypal Kondo lattice compounds $CeAl_3$, $CeCu_6$ (Ref. 27) and also in Kondo lattice antiferromagnet $(CePd_3)_8M$ (M=Ga, Ge, and Al).[7,8,12] The resistivity does not apparently exhibit any anomaly at $T_C \sim 35$ K because its large negative temperature coefficient masks the decrease in resistivity occurring due to the ordering of Mn ions (3 mol %). It is interesting to recall that the resistivity of $CePd_3$ also shows a negative temperature coefficient and peaks around 130 K.[22] Qualitatively the peak temperature varies inversely with the characteristic Kondo/spin fluctuation temperature. Therefore, there is a significant reduction of the Kondo temperature in $(CePd_3)_8Mn$. However, compared to Kondo lattices $(CePd_3)_8M$ (M =Ga, Ge, In, and Al)[7,9–11] which all order antiferromagnetically between 1.5 and 8 K, the RKKY interaction is not strong enough to induce magnetic ordering in $(CePd_3)_8Mn$.

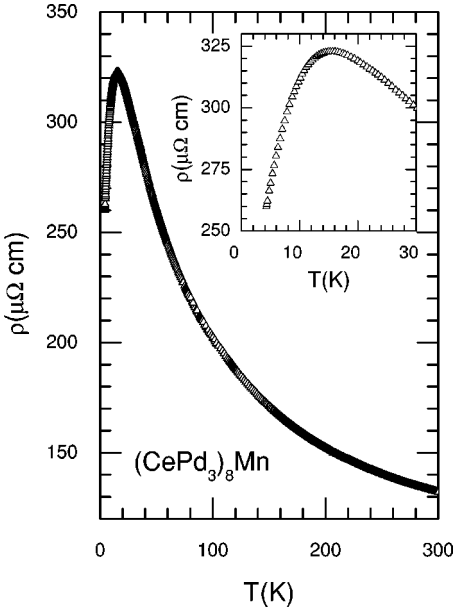

FIG. 12. The resistivity of $(CePd_3)_8Mn$ as a function of temperature. Inset: an enlarged view of the same in low temperatures.

The heat capacity of $(CePd_3)_8Mn$ though comparable to that of the La analog is, however, larger in the entire temperature range of 1.5 to 60 K. This is understandable as the predominant (at higher temperatures) lattice contribution will be nearly similar in the two compounds (the atomic masses of La and Ce differ by less than 1%) but there will be an additional $4f$-derived contribution C_{4f} due to the Ce ions in

$(CePd_3)_8Mn$. The magnetic contribution to the heat capacity C_{mag} (which is predominantly C_{4f} considering that the Mn concentration is low), was derived by subtracting the heat capacity of $(LaPd_3)_8Ga$ from $(CePd_3)_8Mn$. C_{mag} displayed in Fig. 13(a) exhibit a peak at ~ 32 K which we attribute to the ferromagnetic ordering of the Mn sublattice. The peak position of C_{mag} is in agreement with the estimate of the Curie temperature derived from Arrott plots. The inset of Fig. 13 shows C_{mag}/T vs T^2 below 5 K. A linear extrapolation to $T=0$ K gives an intercept of 2.2 J/mol K^2 (275 mJ/Ce mol K^2). In the case of Ce compounds the screening of Ce magnetic moments by the Kondo interaction results in an enhanced coefficient of the electronic specific heat γ. The large value of C_{mag}/T at $T=0$ K shows that $(CePd_3)_8Mn$ is a dense Kondo lattice. We may recall that γ of $CePd_3$ is ~ 50 mJ/mol K2. The hybridization of Ce $4f$ states with the conduction electrons is reduced in the ternary compound thereby leading to a narrow band density of states and an enhanced effective mass. There is no signature of the magnetic ordering of Ce ions in $(CePd_3)_8Mn$ unlike $(CePd_3)_8M$ (M=Ga, Ge, In, Sn, Sb, Bi, and Al)[7,8,12] where the heat capacity exhibits huge peaks between 1.5–10 K.

IV. SUMMARY

We have synthesized and studied the magnetic, thermodynamic, and magnetotransport properties of two interstitial ''dilute-Mn'' compounds $(LaPd_3)_8Mn$ and $(CePd_3)_8Mn$. The Mn ions in these compounds form a regular sublattice and undergo long-range magnetic ordering. The peculiarity of the antiferromagnetic state in $(LaPd_3)_8Mn$ is reflected in the occurrence of two peaks (at 48 and 23 K) in its low field magnetization and an unusually strong field-induced shift of the lower peak ($T2$) towards $T=0$ K at relatively low fields. Concomitantly, a metamagnetic transition is seen in the magnetization in the ordered state, which is also clearly reflected in the magnetotransport data. The magnetic ordering due to Mn sublattice is ferromagnetic in $(CePd_3)_8Mn$, though the Ce sublattice shows dense Kondo lattice behavior and remains paramagnetic at least down to 1.5 K. It would be interesting to probe the magnetic behavior of $(LaPd_3)_8Mn$ in the vicinity of the metamagnetic field at very low temperatures.

ACKNOWLEDGMENT

We thank Dr. Pratap Raychaudhuri for useful discussions.

*Electronic address: surjeets@tifr.res.in
†Electronic address: sudesh@tifr.res.in

[1] S.K. Dhar, S. Malik, and R. Vijayraghvan, Mater. Res. Bull. **16**, 1557 (1981).
[2] S.K. Malik, R. Vijayraghvan, E.B. Boltich, R.S. Craig, W.E. Wallace, and S.K. Dhar, Solid State Commun. **43**, 243 (1982).
[3] S.K. Dhar, S.K. Malik, and R. Vijayraghvan, Phys. Rev. **24**, 6182 (1981).
[4] S.K. Dhar, S.K. Malik, D. Rambabu, and R. Vijayraghvan, J. Appl. Phys. **53**, 8077 (1982).
[5] S.K. Dhar, R. Nagarajan, S.K. Malik, R. Vijayaraghavan, M.M. Abd-Elmeguid, and H. Micklitz, Phys. Rev. B **29**, 5953 (1984).
[6] R.A. Gordon and F.J. DiSalvo, Z. Naturforsch. B **51**, 52 (1996).
[7] S. Singh and S.K. Dhar, J. Phys.: Condens. Matter **14**, 11 755 (2002).
[8] R.A. Gordon, C.D.W. Jones, M.G. Alexander, and F.J. DiSalvo, Physica B **225**, 23 (1996).
[9] B. Cho, R.A. Gordon, C.D.W. Jones, F.J. DiSalvo, J.S. Kim, and G. Stewart, Phys. Rev. B **57**, 15 191 (1998).
[10] C.D.W. Jones, R.A. Gordon, B.K. Cho, F.J. DiSalvo, J.S. Kim, and G. Stewart, Physica B **262**, 284 (1999).
[11] C. Mitra, S.K. Dhar, S. Ramakrishnan, and N.G. Patil, Physica B **259–261**, 108 (1999).
[12] C. Mitra, S.K. Dhar, and S. Ramakrishnan, Solid State Commun. **110**, 701 (1999).
[13] J.Y. Chan, S.M. Kauzlarich, P. Kalvins, R.N. Shelton, and D.J. Webb, Phys. Rev. B **57**, R8103 (1998).
[14] J.Y. Chan, M.M. Olmstead, S.M. Kauzlarich, and D.J. Webb, Chem. Mater. **10**, 3583 (1998).
[15] I.R. Fisher, T.A. Wiener, S.L. Bud'ko, P.C. Canfield, J.Y. Chan, and S.M. Kauzlarich, Phys. Rev. B **59**, 13 829 (1999).
[16] FULLPROF x-ray powder diffraction program available at ccp14, URL: www.ccp14.ac.uk
[17] P. Scoboria, J.E. Crow, and T. Mihalisin, J. Appl. Phys. **50**, 1895 (1979).
[18] R.S. Perry *et al.*, Phys. Rev. Lett. **86**, 2661 (2001).
[19] S.A. Grigera, R.S. Perry, A.J. Schofield, M. Chiao, S.R. Julian, G.G. Lonzarich, S.I. Ikeda, Y. Maeno, A.J. Millis, and A.P. Mackenzie, Science **294**, 329 (2001).
[20] S. Singh and S.K. Dhar, the detailed results based on dc magnetization, ac susceptibility, heat capacity, and resistivity on $LaPd_3Mn_x$ and $CePd_3Mn_x$ ($x=0.03,0.06$) are to be published elsewhere.
[21] W.E. Gardner, J. Penfold, T.F. Smith, and I.R. Harris, J. Phys. F: Met. Phys. **2**, 133 (1972).
[22] M.J. Besnus, J.P. Kappler, and A. Meyer, J. Phys. F: Met. Phys. **13**, 597 (1983).
[23] E. Holland-Moritz, M. Loewenhaupt, W. Scmatz, and D.K. Wohlleben, Phys. Rev. Lett. **38**, 983 (1977).
[24] E. Holland-Moritz, D.K. Wohlleben, and M. Loewenhaupt, Phys. Rev. B **25**, 7482 (1982).
[25] L. Néel, Ann. Phys. (Leipzig) **4**, 249 (1949).
[26] S. Süllow, I. Prasad, M.C. Aronson, S. Bogdanovich, J.L. Sarro, and Z. Fisk, Phys. Rev. B **62**, 11 626 (2000).
[27] G.R. Stewart, Rev. Mod. Phys. **56**, 755 (1984).